Polymer-Coated Carbon Nanotubes as a Molecular Heater Platform for Hyperthermic Therapy

Koichiro Mori[1, 2)] , Minoru Kawaguchi[2, 3)] , Tsuyohiko Fujigaya[4, 5)] , Jun Ohno[2)] and Tetsuro Ikebe[1)]

[1)] *Department of Oral and Maxillofacial Surgery, Fukuoka Dental College, Fukuoka, Japan*
[2)] *Center for Regenerative Medicine, Fukuoka Dental College, Fukuoka, Japan*
[3)] *Department of Dental Engineering, Fukuoka Dental College, Fukuoka, Japan*
[4)] *Department of Applied Chemistry, Graduate School of Engineering, Kyushu University, Fukuoka, Japan*
[5)] *International Institute for Carbon-Neutral Energy Research (WPI-I2CNER), Kyushu University, Fukuoka, Japan*

Correspondence to: Dr. Koichiro Mori, Department of Oral and Maxillofacial Surgery, Fukuoka Dental College, Tamura2-15-1, Sawara-ku, Fukuoka, 814-0193 Japan; Tel: +81-92-801-0411; Fax: +81-92-801-4909; E-mail: mori@college.fdcnet.ac.jp

Running Title
Polymer-coated carbon nanotubes for a hyperthermic therapy

Abstract: Carbon nanotubes have been explored as heat-delivery vehicles for thermal ablation of tumors. To use single-walled carbon nanotubes (SWNT) as a “molecular heater” for hyperthermic therapy in cancer treatment, stable dispersibility and smart-targeting potential are necessary. The current study reports the dispersibility and exothermic properties with near-infrared (NIR) exposure for SWNT coated with a copolymer of *N*-isopropylacrylamide and polyethyleneglycol methacrylate (SWNT/PNIPAM-PEG-hybrid). The SWNT/PNIPAM-PEG hybrid showed stable dispersibility in PBS solution and exothermic potential with NIR exposure. Raman spectroscopy results revealed a hybrid-derived Raman peak in mouse liver and spleen lysates for 7 days post-injection that disappeared by 14 days in all tissues (liver, spleen, heart, lung and kidney). These results suggested that the hybrid did not accumulate in mouse organ tissues in the long-term. The SWNT/PNIPAM-PEG hybrid decreased the cell viability (of mouse macrophages) with heat generation by NIR exposure. The results of this study demonstrate that the SWNT/PNIPAM-PEG hybrid is a useful platform for a “molecular heater” applicable to hyperthermic cancer therapy.

Keywords: Carbon nanotubes, Hyperthermia, Biodistribution, Raman spectra

Introduction

Carbon nanotubes (CNTs) have a wide range of potential for biomedical applications, including biosensors, biomolecular recognition devices and molecular transporters, and cancer therapy and diagnosis[1-8]. For cancer therapeutics, CNTs have extraordinary photothermal energy conversion efficiency and high absorption cross-sections in wavelength ranges capable of transmission within the diagnostic window. Although other nanomaterials, such as gold nanoparticles, also have these photothermal properties[9], CNTs can be more effectively heated due to their strong absorbance in the near-infrared (NIR) region[10]. This exothermic generation potential by NIR irradiation can be used for hyperthermic cancer treatment[11]. The release of this energy within a tissue produces localized heating, which can be exploited to destroy cancer cells[12, 13].

To achieve good performance with a CNT-based nano-heating device, stable and sufficient dispersibility of CNTs into body fluids and selective targeted cell-attachment ability of the CNTs are necessary. In our previous studies, the single-walled carbon nanotube (SWNT) was functionalized with double-stranded DNA to improve its dispersibility, and a complex composed of the DNA-functionalized SWNT and an antibody was prepared[14, 15]. This complex (DNA-SWNT antibody complex) showed good selectivity in binding to the targeted protein, and may be useful as a smart

“molecular heater” platform applicable to various types of antibodies targeting specific antigens. To prepare the DNA-SWNT antibody complex, the SWNT was treated with strong acid prior to DNA functionalization. Although this acid treatment of SWNT can improve the hydrophilicity by formation of a surface carboxylic group, the primary SWNT structure was broken into fragments with shorter lengths. Such structural defects affect many unique features including specific properties in the NIR region, which may decrease the potential for use in thermal ablation. Furthermore, the broken fragments having a wide range of lengths may affect the long-term fate of the SWNT *in vivo*.

A novel treatment method for SWNT with controlled length and a native side-wall structure was recently reported by Tsutsumi et al.[16-18]. The SWNT/polymer hybrid prepared by this method was coated with highly stable SWNT/ultrathin cross-linked polymer (poly *N*-isopropylacrylamide: PNIPAM) networks and is useful for biomedical applications. Furthermore, introducing an additional functional group in the PNIPAM network structure on the SWNT (polyethyleneglycol methacrylate as the co-monomer) allows the fabrication of more stable SWNT/polymer hybrids (SWNT/PNIPAM-PEG hybrid). The intact side-wall structure of the SWNT/PNIPAM-PEG hybrid is an advantageous feature for thermal ablation induced by NIR exposure. Additionally, a hybrid with controllable tube length offers good potential because individual tubes of a

suitable size (below 1 μm in length) are necessary when considering the toxicity[19, 20]. Thus, the SWNT/PNIPAM-PEG hybrid may be highly suitable as a molecular heater platform for cancer photothermal therapy.

The purpose of this study was to evaluate the potential of the SWNT/PNIPAM-PEG hybrid for use as a molecular heater platform. We investigated the stability of dispersal and thermal ablation efficiency of SWNT/PNIPAM-PEG hybrids under biological conditions. To assess the biodistribution of the hybrid injected intravenously in mice, accumulation in various organs was investigated by Raman spectrum measurement. Furthermore, cell viability assessment was carried out when the SWNT/PNIPAM-PEG hybrid attached to mouse macrophages, to clarify the effect of NIR-induced thermal ablation.

Materials and methods

Preparation of SWNT/PNIPAM-PEG hybrids

The SWNT/PNIPAM-PEG hybrids were prepared according to the previously described method[18]. Briefly, SWNT (6 mg, HiPco, Carbon Nanotechnologies, Houston, Texas, USA) was dispersed in a 0.2 wt% sodium dodecyl sulfate aqueous solution (60 ml) by ultrasonication for 1 h, then centrifuged at 60,000 g (Hitachi himac, CS150 GX)

for 1h. The top 90 % of the supernatant solution was collected and sonicated for a further 30 min. *N*-Isopropylacrylamide (NIPAM, 130 mg) and *N*,*N*'-methylenebisacrylamide (BIS, 10 mg) were added to the solution (25 ml) and then the mixture was bubbled with N_2 gas for 1 hour to remove any residual oxygen. After adding a 20-wt% aqueous solution of ammonium persulfate (29 μl) to the mixture, the polymerization was carried out by heating at 70°C for 7 h. The obtained solution was filtered using a membrane filter (molecular weight cut-off: MWCO = 10,000) to remove excess amounts of SDS molecules and the unreacted monomers.

Preparation of DNA-SWNT

The DNA-functionalized SWNT (DNA-SWNT) was prepared according to the previously described method for comparison[14]. The strong acid treatment (ultrasonication for 7 h in a mixture of sulfuric acid and nitric acid) was carried out to achieve hydrophilicity of the SWNT (acid-treated SWNT). For further stable dispersibility in body fluids, the acid-treated SWNT (10 mg) was functionalized with double-stranded DNA (100 mg, derived from salmon testis, average 300-bp, Maruha-Nichiro Holdings, Tokyo, Japan) in water (10 ml) by ultrasonication for 1 h (DNA-SWNT).

Transmission electron microscopy (TEM) and atomic force microscopy (AFM) observation.

The dispersed SWNT particles in deionized water for each sample were dried on 400-mesh copper grids coated with carbon. The particle morphology and structure of the SWNT samples (acid-treated SWNT, DNA-SWNT, and SWNT/PNIPAM-PEG) were analyzed by TEM (JEM 2000FX, JEOL, Tokyo, Japan). AFM images were also captured using a probe microscope (5500AFM, Agilent, Santa Clara CA, USA and Shimadzu, SPM-9600, Kyoto, Japan) equipped with a SiN probe having a spring constant of 10-130 N/m in tapping mode.

Dispersibility assessment

Phosphate buffered saline (PBS) solutions containing different concentrations of the SWNT (SWNT/PNIPAM-PEG and the DNA-SWNT, 0.01, 0.1, 0.25, and 0.5 mg/ml) were prepared. These solutions (1 ml) were centrifuged at 6,600 rpm for 5 min at 1, 10, 24, and 48 h after being prepared. The supernatant of the centrifuged sample was measured in transmittance mode at 500 nm by ultraviolet-visible spectroscopy (V-560 spectrophotometer, Jasco, Tokyo, Japan), and the change in transmittance was determined

for evaluation of the stability of the dispersed SWNT.

Photothermal properties of the SWNT-containing solution.

PBS solution (1 ml) containing 0.1 mg of the SWNT/PNIPAM-PEG hybrid and DNA-SWNT was added to each well of a 48-well plate and then irradiated with NIR (4.0 W/cm^2, LA-100 IR, Hayashi, Tokyo, Japan). The light tip of the NIR apparatus was located at a distance of 2 cm from the surface of the medium solution in each well. Each medium solution (n=3) was exposed to NIR light for up to 5 min, and the temperature rise of each solution and the PBS alone were continuously measured using a thermometer (DP-700, RKC, Tokyo, Japan) with a thermo-coupled probe (JB-16, RKC, Tokyo, Japan).

Biodistribution assessment

In the present study, seven-week-old ddY mice were used. All animal experiments were performed in accordance with the ethical guidelines for animal experiments of Fukuoka Dental College. Saline solution (0.2 ml containing 2.0 mg of the SWNT-PNIPAM-PEG hybrid or the DNA-SWNT) was intravenously injected into the tail vein of each mouse. For the biodistribution evaluation of SWNT nanoparticles in organs, tissues of organs (heart, lung, liver, kidney and spleen) were collected at 1, 7 and

14 days post injection. The dissected tissues were solubilized in lysis buffer using a homogenizer. The resultant lysate solutions were subjected to Raman measurement. Three or four mice were used for each time point for the SWNT groups.

Cell viability assessment by NIR-induced thermal ablation

PBS solution (6 ml containing 2 mg of SWNT/PNIPAM-PEG hybrid or DNA-SWNT) was injected into the abdominal cavity of 7-week-old male mice, and 4 ml of sample solution was collected at 5 min post-injection. The sample solutions were centrifuged (1,400 rpm, 3 min) to separate the cellular fraction. Additional PBS (1 ml) was added to the cellular fraction, and the cellular fraction (total cell number, $4\text{-}6\times10^4$ cells/ml) was used to assess cell viability. PBS solution (990 μl) was poured into a well of a 24-well plate, and exposed to NIR light for 20 min (exposure distance, 2 cm). After the exposure, the cell number in 10 μl of the PBS solution was determined using a Cell Counting Kit-8 (Dojindo Molecular Technologies, Kumamoto, Japan) according to the manufacturer's instructions. The cell number in 10 μl of the PBS solution without NIR exposure was determined for comparison. The effect of NIR exposure on the cell viability was evaluated by comparing the cell numbers of the samples with and without NIR exposure.

Raman measurement

To obtain the Raman intensity vs. SWNT concentration calibration data, normalized amounts of SWNT/PNIPAM-PEG hybrid were added to the PBS solution, lysate tissue sample (for biodistribution assessment) and cellular fraction (for cell viability assessment) without the SWNT injection.

Raman spectra of SWNT solutions with known concentrations were taken, and the G-band intensities were plotted against SWNT concentrations as the calibration curve. The Raman spectra were recorded using a Raman spectrophotometer at 785 nm excitation (Kaiser Optical Systems, Raman RXN System) with a 10 s exposure (10-times accumulation). The G-band peak at 1,590 cm^{-1} was used for SWNT detection.

Statistical analysis

Statistical analysis was performed using ANOVA. The statistical significance was analyzed using the Student's *t*-test. A *P*-value of <0.05 was considered to be significant.

Results

Morphology and structural observation of SWNT samples.

A typical TEM image of the acid-treated SWNT is shown in Fig. 1A, in which a highly bundled structure is observed. Fig. 1B shows a TEM image of the DNA-SWNT. The DNA-SWNT was well dispersed with various lengths. The SWNT/PNIPAM-PEG hybrid was well dispersed with shorter lengths, as shown in Fig. 1C.

Fig. 1 (D-F) shows typical AFM images for each SWNT. Although the acid-treated SWNT and the DNA-SWNT display no specific structure, the SWNT/PNIPAM-PEG hybrids with needle-like structures were well dispersed (Fig. 1F).

Dispersibility of SWNT samples.

No aggregated particles were visible in the PBS solutions containing the SWNT/PNIPAM-PEG hybrid and the DNA/SWNT. The transmittance of the PBS solutions containing the SWNT/PNIPAM-PEG hybrid (38% of the transmittance) and the DNA-SWNT (22% of transmittance) did not change even after 24 hours.

In vitro photothermic properties

Thermal generation was observed during the NIR irradiation. The temperatures

of the PBS solutions containing the SWNT/PNIPAM-PEG hybrid and the DNA-SWNT both increased with longer irradiation times (Fig. 2). The temperature increase of the solution was 45°C within 5 minutes of irradiation for SWNT/PNIPAM-PEG hybrid, and was 40°C for the DNA-SWNT. With the same NIR irradiation conditions, the PBS solution containing SWNT/NIPAM-PEG hybrids showed a higher rate of temperature increase than the DNA-SWNT-containing PBS solution.

Raman analysis

The Raman intensity vs. SWNT concentration calibration curve is shown in Fig. 3. The linear dependence allowed for quantitative measurement of the SWNT/PNIPAM-PEG hybrid in PBS solution (Fig. 3A). For the PBS solution with cellular fraction, linear dependence was observed from 0.002 mg/ml to 0.04 mg/ml (Fig. 3B). Thus, quantitative analysis of SWNT with Raman spectra was carried out to assess the biodistribution and cell viability of the SWNT/PNIPAM-PEG hybrid（Fig. 3C and 3D）. However, for the DNA-SWNT sample, the data for the calibration curve could not be measured because sufficient intensity of the Raman signal was not detected.

Biodistribution assessment

Fig. 4 shows Raman spectra of liver (A) and spleen (B) lysates at 1 day, 7 days and 14 days post injection. At 1 day post-injection, the G-band peak of SWNT was detected only from the liver sample (0.105 mg of calculated SWNT). At 7 days post-injection, the G-band peak was detected from the liver (0.180 mg of calculated SWNT) and spleen (0.006 mg of calculated SWNT) samples for the SWNT/PNIPAM-PEG hybrid injected mice. However, no detectable G-band peak was seen in any organ at 14 days post-injection. For the DNA-SWNT injected mice, no detectable G-band peak was observed in any organ (data were not shown). The measured %ID(percentage of injected dose) of SWNT/PNIPAM-PEG (Fig. 4C) values were approximately 53 and 93% of the injected hybrid (total amount of the hybrid for the liver and spleen sample at the same time point) at days 1 and 7 post-injection, respectively.

Cell viability assessment

As shown in Fig. 5(A), cell viability was decreased by NIR exposure when attached with the SWNT/PNIPAM-PEG hybrid ($p<0.05$). A typical Raman spectrum is shown in Fig. 5(B) for the centrifuged cellular fraction and the supernatant of the SWNT/PNIPAM-PEG hybrid sample. The concentration of the hybrid in cellular fraction showed a higher value (8.0 ± 0.5 μg/ml) than that of the supernatant of the centrifuged

sample solution (5.0 ± 0.5 μg/ml) collected from mice ($p<0.05$). There was no significant difference in cell viability between the cellular fraction with or without NIR exposure for the control group ($p>0.05$). The cell viability with DNA-SWNT attached showed a similar NIR exposure result. However, the concentration of the DNA-SWNT could not be determined because no G-band peak was observed.

Discussion

To achieve good performance of a SWNT-based molecular heating device for hyperthermic cancer therapy, two main approaches should be discussed: 1) improve the solubility for stable and sufficient dispersibility of the SWNT in body fluids, and 2) enable selective targeted cell attachment of the SWNT by surface functionalization. In this study, we described the potential of the SWNT/PNIPAM-PEG hybrid as a base model for a molecular heating device to improve the stability of dispersal in body fluids.

Although water-soluble DNA-SWNT was obtained by strong acid oxidation that generates –OH and –COOH groups on the graphitic SWNT surface[14], such generated structural defects detrimentally affect many unique features of SWNT including specific optical properties in the NIR region. In contrast, the SWNT/PNIPAM-PEG hybrid was prepared by ultrathin crosslinked polymer coating (~nm-size) of the pristine-SWNTs, and

subsequent ultracentrifugation to limit the length of the hybrid[17]. Thus, the obtained SWNT/PNIPAM-PEG hybrid has two unique properties: controlled tube length and an intact surface graphitic structure. The intact surface structure of the SWNT/PNIPAM-PEG hybrid retains its exothermic efficiency in response to NIR irradiation even after coating the surface with PNIPAM-PEG copolymer. Indeed, as shown in Fig. 2, the SWNT/PNIPAM-PEG hybrid showed a rapid temperature increase with NIR exposure, at a higher rate of increase than the DNA-SWNT.

For therapeutic application of SWNT-based nanoparticles, the SWNT biodistribution profile after administration into animals should be addressed. From the results of biodistribution experiments using radiolabeled SWNTs, SWNTs showed high uptake in the liver and spleen with low urinary excretion[21]. Although the radiolabeling method is a convenient way to determine the biodistribution of SWNTs, excess free radioisotopes in the radiolabeled SWNT samples may lead to false results. In contrast, the intensity of the G-band of SWNTs' Raman spectrum is relatively insensitive to the diameter and bundling nature of SWNTs. Furthermore, Raman spectroscopy can be used to detect SWNTs in animals with high fidelity, without the concern of radiolabeling falling off or decaying over time[2]. We thus used Raman spectroscopy to probe the biodistribution of SWNTs in various organs of mice. As shown in Fig. 3, a sharp Raman spectrum G-

band peak was observed, and its linear dependence allowed for quantitative measurement of the SWNT/PNIPAM-PEG hybrids' concentrations in PBS solution. However, PBS solutions of the same concentrations of DNA-SWNT showed no sharp G-band peak. This may be due to the partially destroyed surface structure of the DNA-SWNT. Liu et al. [22] evaluated the biodistribution of SWNT functionalized by branched polyethyleneglycol (PEG) chains in mice over a period of three months by Raman spectrum measurement. They found that hydrophilic functionalization, such as the PEG coatings, resulted in biologically inert SWNTs with long blood circulation, low RES (reticuloendothelial system) uptake, and relatively fast clearance from organs. Although they detected the G-band peak in lysate tissues (liver and spleen) even 3 months after injection, the SWNT concentrations in other organs (such as heart, lung and kidney) were below detection limits. We detected the G-band peak in liver and spleen lysates for up to 7 days post-injection, but no appreciable Raman signals were detected in heart, lung or kidney tissues (Fig. 4). The Raman signal at 14 days post injection was not detectable for either the liver or spleen tissues. The total amount of the hybrid determined from the Raman signals for the liver and spleen (7 days) indicated that approximately 95% of the hybrid was excreted within the first 7 days after injection. Although these findings do not mean the absence of SWNT/PNIPAM-PEG hybrid accumulation in these organs after 14 days post-injection,

it is possible that the hybrid is rapidly excreted from the mouse body. As shown by several biodistribution studies of SWNTs, appropriately functionalized SWNTs with hydrophilic and biocompatible coatings are stable in biological environments, with minimal toxicity in vivo. The PNIPAM used as the coating polymer for SWNT in this study is a well-known temperature-responsive and biocompatible polymer. Thus, intravenously-injected SWNT/PNIPAM-PEG hybrids may show stable blood circulation and excretion without long-term accumulation in organs.

Thermal ablation above 55°C leads to coagulative necrosis and protein denaturation of malignant cells due to the local increase in temperature[23, 24]. We evaluated the effect of NIR-induced heat generation of the hybrids on the viability of mouse macrophages (instead of cancer cells). The cell viability decreased when NIR irradiation was applied with the SWNT/PNIPAM-PEG hybrids. As shown in Fig. 5, the centrifuged cellular fraction collected from mice showed a clear G-band peak. The intensity of this peak was 1.3 times higher than that of the supernatant of the fraction. The difference in concentration of the hybrid between the centrifuged cellular fraction and the supernatant suggested that the injected hybrid attaches to cells. Although it is not clear whether the hybrid was attached to the surface of the cells or incorporated into the cells by endocytosis,

this decrease in cell viability may be due to the thermal ablation cell death induced by the SWNT/PNIPAM-PEG hybrids.

As mentioned above, the cross-linked PNIPAM-PEG coating did not affect the heat generation efficiency of the SWNT/PNIPAM-PEG hybrid. It is possible that if a monomer with functional groups, such as hydroxy, carboxyl, or imido groups, was copolymerized with the PNIPAM-PEG, these functional groups may be introduced into the polymer coating layer. Ligands corresponding to the targeted protein can be introduced into the polymer coating layer via these functional groups. Thus, the hybrid is a useful antibody complex platform applicable for various types of antibodies in response to the corresponding target molecule.

In summary, the SWNT/PNIPAM-PEG hybrid has potential as a nano-platform for molecular heating devices in hyperthermic therapy. The intact side-wall structure, controlled tube length, and surface coating with biocompatible PNIPAM-PEG copolymer make the hybrid highly stable under biological conditions. Furthermore, the hybrid showed suitable heat generation by NIR exposure, capable of inducing cell death. Although quantitative evaluation of the biodistribution in vivo could not be conducted, the hybrid did not show long-term accumulation in mouse organ tissues. The

SWNT/PNIPAM-PEG hybrid is an appropriate molecular heating platform for hyperthermic devices.

Acknowledgment

The authors acknowledge Dr. Yusuke Tsutsumi and Ms.Yukiko Nagai (Department of Applied Chemistry, Graduate School of Engineering, Kyushu University), and Dr. Naotoshi Nakashima (International Institute for Carbon-Neutral Energy Research.WPI-I2CNER Kyushu University) for help with Raman analysis. This study was supported by JSPS KAKENHI Grant Number 16K11641.

Conflict of Interest

The authors have declared that no COI exists.

References

1. Liu Z, Chen K, Davis C, Sherlock S, Cao Q, Chen X and Dai H. Drug delivery with carbon nanotubes for in vivo cancer treatment. Cancer Res 68: 6652-6660, 2008
2. Liu Z, Tabakman S, Welsher K and Dai H. Carbon Nanotubes in Biology and Medicine: In vitro and in vivo Detection, Imaging and Drug Delivery. Nano Res 2: 85-120, 2009
3. DaSilva EE, Colleta HH, Ferlauto AS, Moreira RL, Resende RR, Oliveira S, Kitten GT, Lacerda RG and Ladeira LO. Nanostructured 3-D collagen/nanotube biocomposites for future bone regeneration scaffolds. Nano Res 2: 462-473, 2009
4. Bhirde AA, Patel S, Sousa AA, Patel V, Molinolo AA, Ji Y, Leapman RD, Gutkind JS and Rusling JF. Distribution and clearance of PEG-single-walled carbon nanotubes cancer drug delivery vehicles in mice. Nanomedicine 5: 1535-1546, 2010
5. Welsher K, Sherlock S P and Dai H. Deep-tissue anatomical imaging of mice using carbon nanotube fluorophores in the second near-infrared window. Proc Natl Acad Sci USA 108: 8943-8948, 2011
6. Kawaguchi M, Mori K, Kajiya H, Ikebe T and Fukushima T. In vivo evaluation of bone regeneration by DNA/protamine complex treatment with photothermal stress stimulation in an aged rat calvarial defect model. J Oral Tissue Engin 13: 67-76, 2015
7. Asha ML, Ghorai L, Rajarathnam BN, Kumar HMM, Lekshmy J and Jasti S.

Carbon nanotubes: a novel approach for cancer diagnosis and therpy. J Orofac Res 5: 84-89, 2015
8. Son KH, Hong JH and Lee JW. Carbon nanotubes as cancer therapeutic carriers and mediators. Int J Nanomed 11: 5163-5185, 2016
9. Abadeer NS and Murphy CJ. Recent progress in cancer thermal therapy using gold nanopaerticles. J Phys Chem 120: 4691-4716, 2016
10. Robinson JT, Welsher K, Tabakman S M, Sherlock SP, Wang H, Luong R and Dai H. High Performance In Vivo Near-IR (>1 μm) Imaging and Photothermal Cancer Therapy with Carbon Nanotubes. Nano Res 3: 779-793, 2010
11. Elhissi A M. A. Ahmed W, Hassan IU, Dhanak V R and Emanuele A D. Carbon Nanotubes in Cancer Therapy and Drug Delivery. J Drug Deliv http://dx.doi.org/10.1155/2012/837327, 2012
12. Murakami T, Nakatsuji H, Inada M, Matoba Y, Umeyama T, Tsujimoto M, Isoda S, Hashida M and Imahori H. Photodynamic and Photothermal Effects of Semiconducting and Metallic-Enriched Single-Walled Carbon Nanotubes. J Am Chem Soc 134: 17862–17865, 2012
13. Sobhani Z, Behnam MA, Emami F, Dehghanian A and Jamhiri I. Photothermal therapy of melanoma tumor using multiwalled carbon nanotubes. Int J Nanomed 12: 4509-4517, 2017
14. Kawaguchi M, ohno J, Irie A, Yamazaki J and Nakashima N. Dispersion stability and exothermic properties of DNA-functionalized single-walled carbon nanotubes. Int j Nanomedicine 6: 729-736, 2011
15. Kawaguchi M, Yamazaki J, Ohno J and Fukushima T. Preparation and binding study of a complex made of DNA-treated single-walled carbon nanotubes and antibody for specific delivery of a “molecular heater” platform. Int J Nanomed 7: 4363-4372, 2012
16. Tsutsumi Y, Fujigaya T and Nakashima N. Polymer synthesis inside a nanospace of a surfactant-micelle on carbon nanotubes: creation of highly-stable individual nanotubes/ultrathin cross-linked polymer hybrids. Rsc Adv 4:6318-6323, 2014
17. Tsutsumi Y, Fujigaya T and Nakashima N. Size reduction of 3D-polymer-coated single-walled carbon nanotubes by ultracentrifugation. Nanoscale 7: 19534-19539, 2015
18. Tsutsumi Y, Fujigaya T and Nakashima N. Requirement for the formation of crosslinked polymers on single-walled carbon nanotubes using vinyl monomers. Chem Lett 45: 274-276, 2016
19. Jin H, Heller DA, Sharma R and Strano MS. Size-dependent cellular uptake and

expulsion of single-walled carbon nanotubes: single particle tracking and a generic uptake model for nanoparticles. ACS Nano 3: 149-158, 2009
20. Kang B, Chang S, Dai Y, Yu D and Chen D. Cell response to carbon nanotubes: size-dependent intracellular uptake mechanism and subcellular fate. Small 6: 2362-2366, 2010
21. Singh R, Pantarotto D, Lacerda L, Pastrin G, Klumpp C, Prato M, Bianco A and Kostarelos K. Tissue biodistribution and blood clearance rates of intravenously administrated carbon nanotube radiotracers. Proc Natl Acad Sci USA 103: 3357-3362, 2006
22. Liu Z, Davis C, Cai W, He L, Chen X and Dai H. Circulation and long-term fate of functionalized biocompatible single-walled carbon nanotubes in mice probed by Raman spectroscopy. Proc Natl Acad Sci USA 105: 1410-1415, 2008
23. Kam NW, O'Connell M, Wisdom JA and Dai H. Carbon nanotubes as multifunctional biological transporters and near-infrared agents for selective cancer cell destruction. Proc Natl Acad Sci USA 102: 11600-11605, 2005
24. Madani SY, Naderi N, Dissanayake O, Tan A and Seifalian AM. A new era of cancer treatment: carbon nanotubes as drug delivery tools. Int J Nanomedicine 6: 2963-2979, 2011

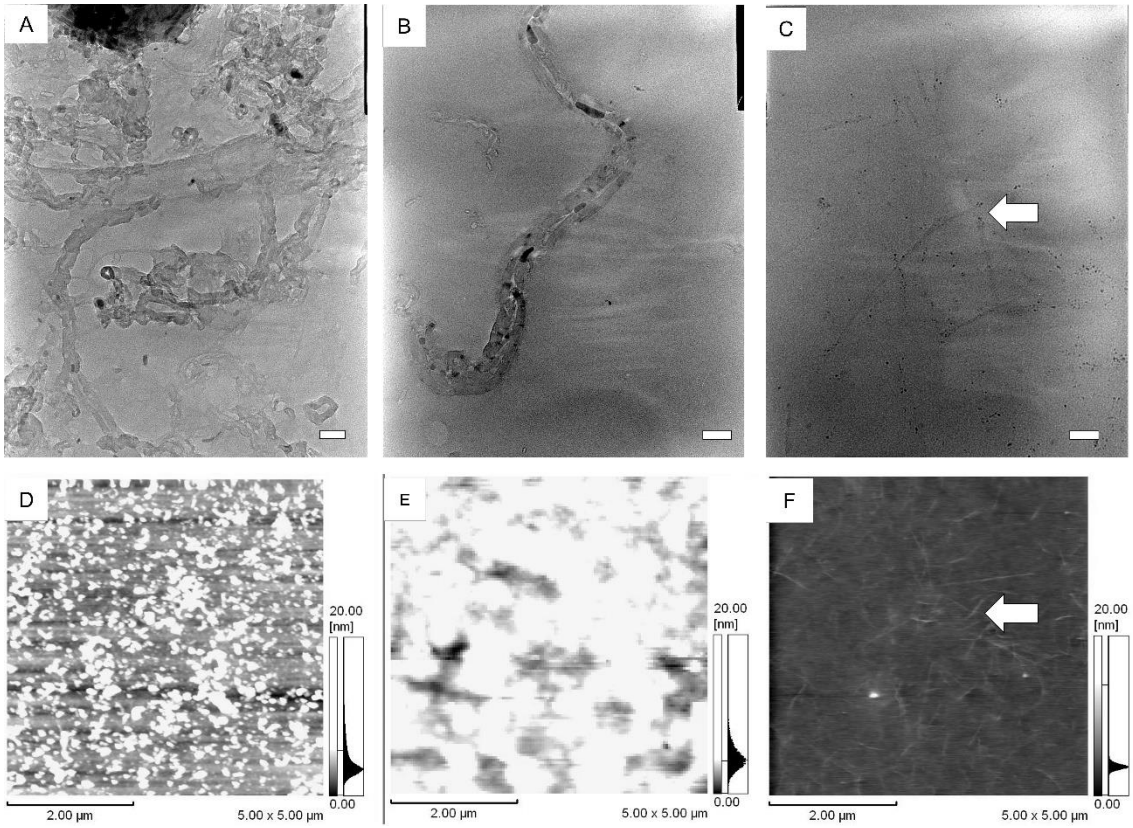

Figure 1. Typical transmission electron microscopy images (upper) and atomic force microscopy images (lower) of the acid-treated SWNT (A and D), the DNA-SWNT (B and E), and the SWNT/PNIPAM-PEG hybrid (C and F).（bar =50 nm in A, B and C）

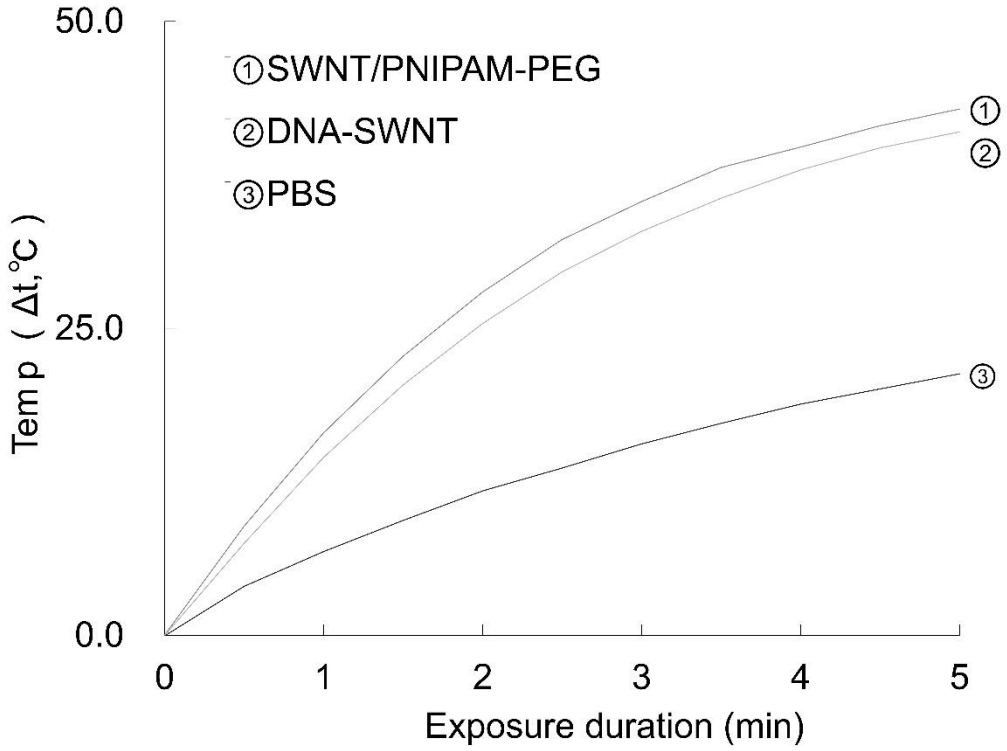

Figure 2. In vitro exothermic heat generation of the SWNT/PNIPAM-PEG and the DNA-SWNT hybrid. The heat generation was dependent on the exposure time to near-infrared (NIR) light.

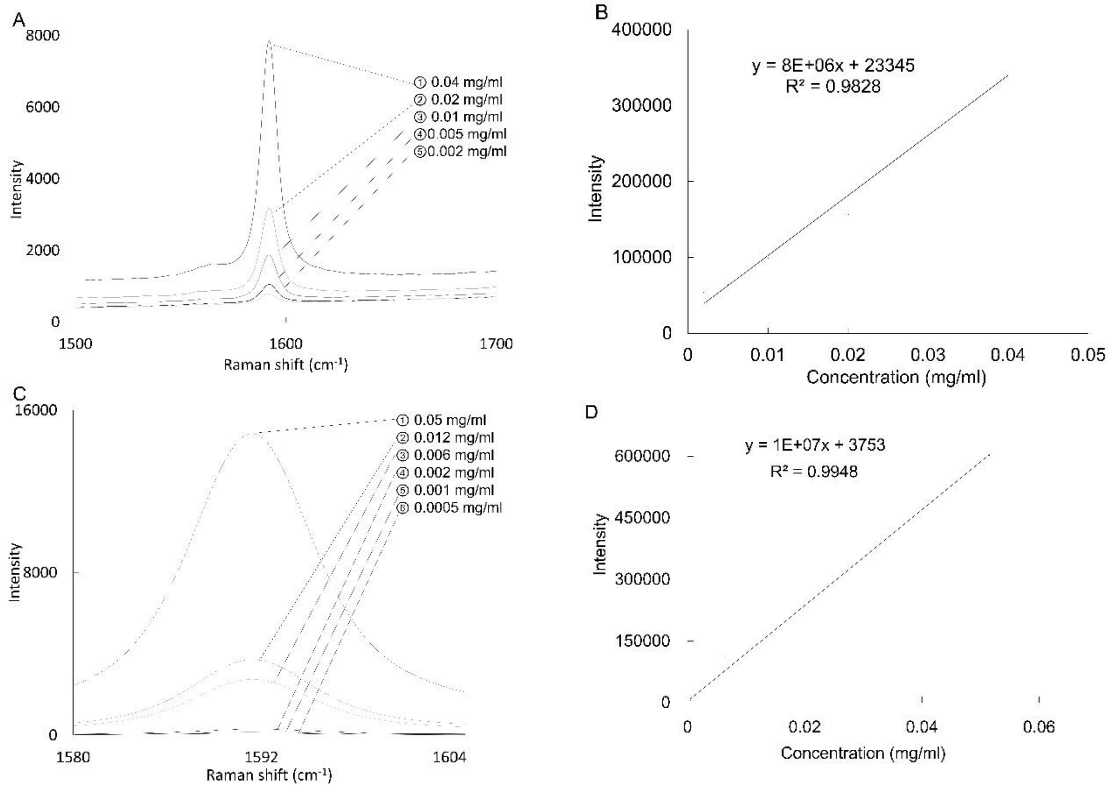

Figure 3. G-band peak at 1,590 cm^{-1} for the SWNT/PNIPAM-PEG hybrid in PBS solution (A) and calibration curve of Raman intensity vs. hybrid concentration (B). G-band peak for the hybrid in PBS solution with the cellular fraction (C) and the calibration curve (D).

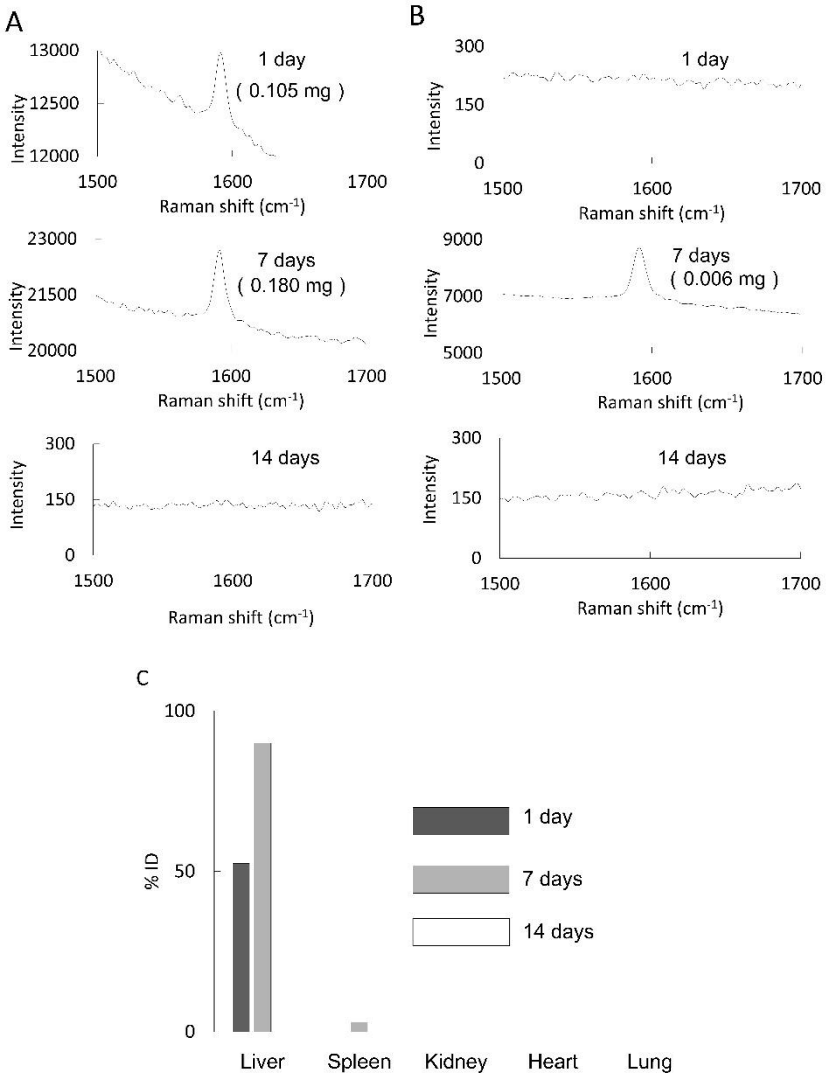

Figure 4. Representative Raman spectra of the SWNT/PNIPAM-PEG hybrid in tissue homogenates of liver (A) and spleen (B), of mice at 1, 7, and 14 days post-injection. The value of %ID (injection dose) for each mouse organ tissue (C).

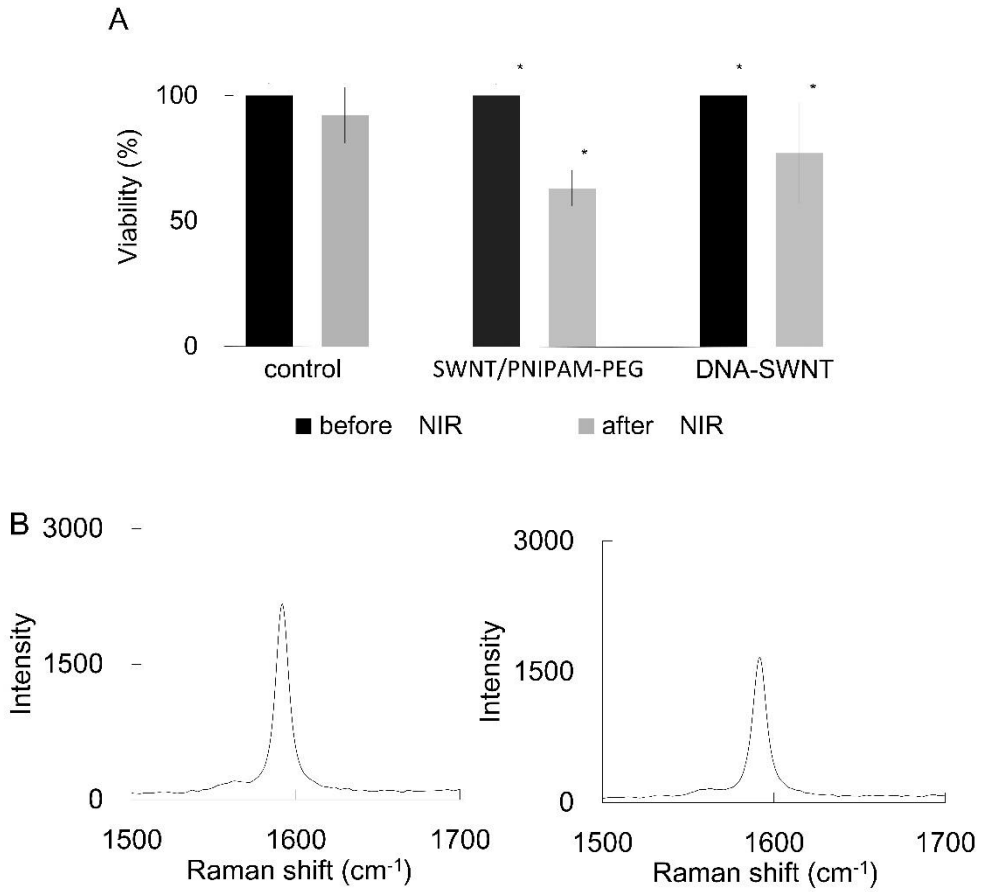

Figure 5. (A) Viability of mouse macrophages exposed to the DNA-SWNT and the SWNT/PNIPAM-PEG hybrid. Asterisk indicates a statistically significant difference compared to the control group (without NIR light exposure). Asterisk shows a significant difference ($p<0.05$) between groups with or without NIR exposure. (B) Typical Raman spectrum of the cellular fraction (left) and the supernatant (right) of the SWNT/PNIPAM-PEG hybrid sample.